Periodic Ridge Formation in Elastic Film-Substrate System

Dengge Jin

Department of Engineering Mechanics, Tsinghua University, Beijing, P.R.C.

Abstract

1. Introduction

2. Morphology evolution: from wrinkling to ridge formation

A neo-Hookean bilayer system consisting of a thin stiff film of thickness h_f lying on a pre-stretched soft substrate of thickness h_s is considered here. To ensure the ridge formation occurs in the compression process, the ground shear moduli ratio of the film to substrate is set to be a large value, $\mu_f / \mu_s = 774$, which is applied to all the simulation cases in this paper. The actual process of pre-stretch and overall compression is illustrated in the schematic in fig.1(a): (a1) first the substrate is pre-stretched uniformly to a prescribed stretch ($\lambda_0 = 1.1 \sim 2.1$); (a2) then the free stressed film is attached on the pre-stretched substrate, the two parts are assumed to be perfectly bonded at the interface; (a3) releasing the substrate, the bilayer system will undergo overall compression ε, leading to wrinkling and subsequent bifurcation.

For the elastic bilayer system, previous works have developed a set of analytical solutions of wrinkling bifurcation. For a neo-Hookean bilayer system with substrate pre-stretched, the solution for critical strain and wave number can not be given directly in an explicit form. When the film is very stiff compared to the substrate, the strain in the film remains small, and it has been demonstrated that in the range of moduli ratio $\mu_f / \mu_s > 100$, the results of linear elastic film on a neo-Hookean substrate is increasingly accurate for the neo-Hookean bilayer. For a linear elastic film on a neo-Hookean substrate which has undergone a uniform pre-stretch λ_0 before attaching to the film, with the plain strain and incompressible condition, the critical strain ε_w for wrinkling and the associated wave number k are

$$\varepsilon_w = \frac{1}{4}\left(\frac{3}{2}\left(1+\lambda_0^2\right)\frac{\mu_s}{\mu_f}\right)^{2/3}$$

$$kh_f = \left(\frac{3}{2}\left(1+\lambda_0^2\right)\frac{\mu_s}{\mu_f}\right)^{1/3} \tag{1}$$

and the wavelength is $l_w = 2\pi / k$, referenced to the undeformed film, and $\lambda_0 l_w$ in the

deformed film. Equation (1) will be used to generate the initial imperfection and to compare with the simulation result.

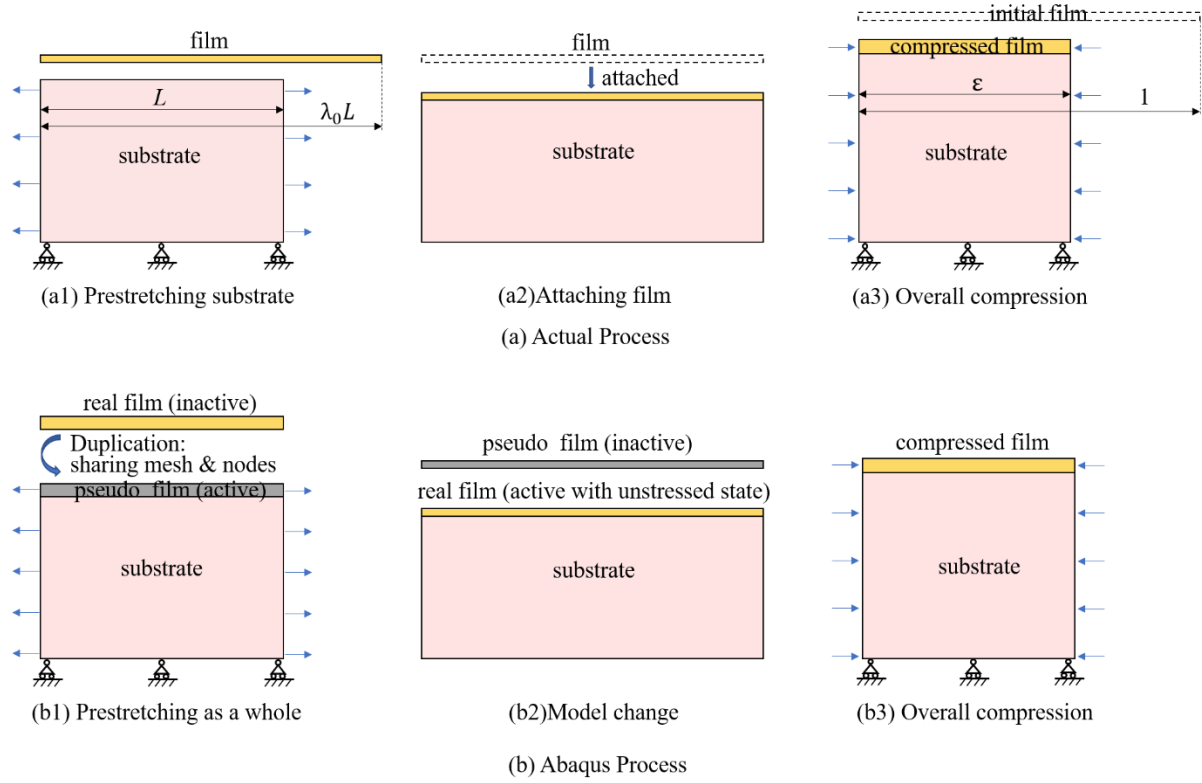## 2.1 Finite element model and Pseudo-dynamic method

film

L

$\lambda_0 L$

substrate

(a1) Prestretching substrate

film

attached

substrate

(a2)Attaching film

initial film

compressed film

ε

1

substrate

(a3) Overall compression

(a) Actual Process

real film (inactive)

Duplication: sharing mesh & nodes

pseudo film (active)

substrate

(b1) Prestretching as a whole

pseudo film (inactive)

real film (active with unstressed state)

substrate

(b2)Model change

compressed film

substrate

(b3) Overall compression

(b) Abaqus Process

Fig.1 Schematic of pre-stretch process by Abaqus "model change" function and overall compression process by pseudo-dynamic method.

Two-dimensional finite element models are employed to simulate the pre-stretch, overall compression and surface morphology bifurcations of the bilayer system, using commercial software Abaqus. The vertical dimensions of the model are normalized by the film thickness h_f and the horizontal dimensions are normalized by associated wavelength $l_w = 2\pi / k$. Specifically, before pre-stretch, the substrate thickness is $h_s = 100 h_f$, which is sufficiently large to avoid specific case; and series of model length, as $L = 10,20,30 l_w$, are chosen to check the consistency of results. On the left and right edges, the shear tractions are zero and a prescribed uniform horizontal displacement is imposed to create the pre-stretch or overall

compression; On the bottom surface of the substrate, the shear tractions and the vertical displacement are zero; and the surface of the film is traction free.

The film and substrate are modeled as hyperelastic by the incompressible neo-Hookean material model, and the ground shear moduli ratio is $\mu_f / \mu_s = 774$ as mentioned before. The 8-node biquadratic plane strain elements CPE8RH with hybrid formulation and reduced integration are used to mesh the model. Structured meshes are generated for both the film and substrate to avoid any perturbation from the uneven mesh. The numerical convergence study was performed to decide the mesh density. Four layers of elements are generated across the film thickness and 100 elements are generated per wavelength along the length.

To intrigue wrinkling and subsequent bifurcation, small imperfections are introduced in the finite element model using the first eigen modes, the sinusoidal wrinkle mode from a linear perturbation analysis of the bilayer system, with amplitude $\Delta_{imp} = 1/50 h_f$. The pseudo-dynamic method is used in the overall compression process. In pseudo-dynamic method, an artificial damping is introduced as a computational ploy that stabilizes the unstable transition from wrinkles to ridges, allowing the computation to pass through the snapping process. The damping factor adopted in this paper is 0.0002, a value suggested by previous researchers.

It should be pointed out that the pre-stretch and film attaching process in Abaqus is different with the actual process. The Abaqus process includes following key steps (fig.1 (b)): (b1) generate a "pseudo film" which is duplicated from the real film and shares the same mesh and nodes with real film. The ground moduli of pseudo film is sufficient small compared to μ_s, while that of real film takes the value of μ_f. The bottom faces of real film and pseudo film are bonded to the upper surface of substrate; (b1) Activate the pseudo film mesh and deactivate the real film, and then pre-stretch the bilayer to a pre-scribed stretch λ_0. As the pseudo film has very small moduli, it almost has no influence in the stretch of substrate, and the stretched deformation of the bilayer is uniform; (b2) Activate the real film with free stress state and deactivate pseudo film by Abaqus "Model change". In this way, the real film mesh, sharing mesh and nodes with the pseudo film, is compatible with the pre-stretched substrate mesh; (b3) With real film activated, compress the bilayer by a pre-scribed uniform horizontal

displacement. This step is accomplished by pseudo-dynamic method as described before.

2.2 Typical surface morphology evolution processes

The results of pseudo-dynamic method show that, for the substrate pre-stretch ranging from $\lambda_0 = 1.1$ to $\lambda_0 = 2.1$, the surface morphology evolution of the overall compressed bi-layer system can be classified into three different types. Figures 2-5 depict some typical stages in the surface evolution with $\lambda_0 = 1.5$, 1.53, 1.7 and 2.0, respectively.

(1) $1.1 \le \lambda_0 \le 1.52$: Transition from wrinkling to periodic doubling. The surface first transitions from flat sate to wrinkling state at overall compression $\varepsilon_w = 0.0086$ (fig.2(a)). When the overall compression reaches another critical strain, $\varepsilon_{pd} = 0.37$, period doubling occurs (Fig. 2(c)).
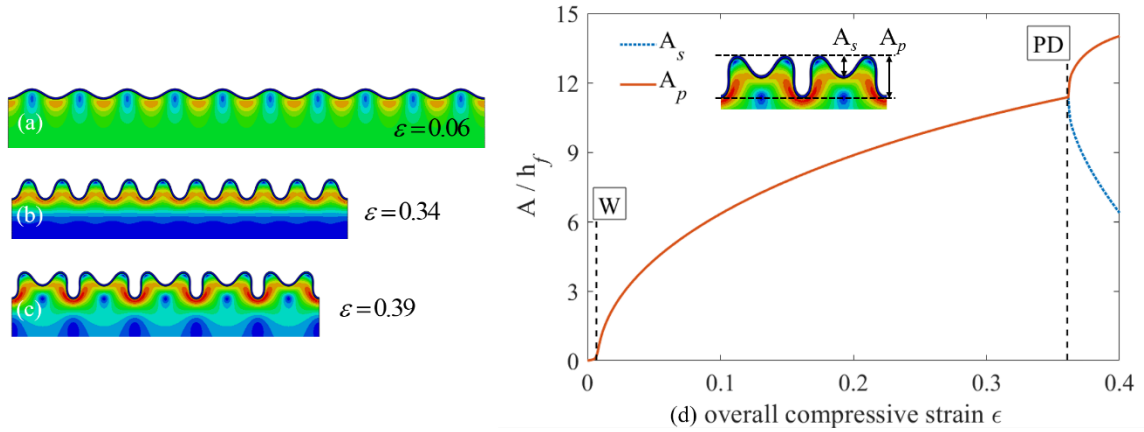

Fig. 2: Wrinkling to period doubling transition in an elastic bilayer system with a prestretch $\lambda_0 = 1.5$. $\varepsilon_w = 0.0086$, $\varepsilon_{pd} = 0.37$. (a)wrinkling state; (b)wrinkling growth; (c)period doubling; (d) evolution of the average depths of the primary and secondary valleys as strain increases. Inset shows the definition of the primary and secondary valley depths.

(2) $1.53 \le \lambda_0 \le 1.9$: Transition from wrinkling to periodic ridge formation, then to second wrinkling and finally to period doubling. Fig.3 and Fig.4 presents two typical evolution process with $\lambda_0 = 1.53$ and $\lambda_0 = 1.7$.

With $\lambda_0 = 1.53$, the surface first transitions from flat sate to wrinkling state at overall

compression $\varepsilon_w = 0.0087$ (fig.3(a)). When overall compression reaches $\varepsilon_{w\to r} = 0.155$, every other wrinkle there is a wrinkle that grows taller, forming periodic small ridges morphosis(fig.3(b)). With increasing overall compression strain, the ridges turn back to the wrinkling state (fig.3(c)) at $\varepsilon_{w2} = 0.188$. The periodic ridges morphosis is transitory throughout the compression process, as it only exists in a small compressive strain range $\varepsilon_{w2} - \varepsilon_{w\to r} \approx 0.033$. The number of wrinkles is the same before and after ridge morphosis. As overall compression increasing, the wrinkles continue to grow (fig.3(d)), and finally transition to period doubling state at $\varepsilon_{pd} = 0.415$ (fig.3(e)).
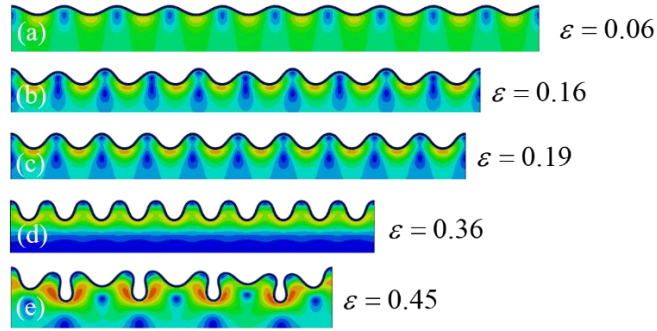

Fig. 3: Wrinkling to periodic ridge formation in an elastic bilayer system with a prestretch $\lambda_0 = 1.53$. $\varepsilon_w = 0.0087, \varepsilon_{w\to r} = 0.155, \varepsilon_{w2} = 0.188, \varepsilon_{pd} = 0.415$. (a)wrinkling state(10 wrinkles); (b)initial periodic ridge formation; (c) second wrinkling(10 wrinkles); (d)wrinkling growth; (e)period doubling.

With $\lambda_0 = 1.7$, when the overall compression increases to the critical strain $\varepsilon_{w\to r} = 0.068$, every 4 wrinkles there is a wrinkle whose height increased dramatically, forming ridges, and the the other wrinkles are flattened(fig.4(b)). These ridges are formed almost simultaneously and periodically, and the initial ridge formation period of $4l_w$ is quite stable with various finite element model size $L = 10, 20, 30l_w$. This process is the initial periodic ridge formation. With increasing overall compression, the height of initial formed ridges increases, however, the growth is limited and new ridges emerge subsequently. In the process of new ridge formation, these ridges are moving to rearrange so that they are always almost equidistant (fig.4(c)),

effectively reducing the space between adjacent ridges. As compression reaches to $\varepsilon_{w2} = 0.26$,

the process of ridge formation and rearangement ends up with a surface morphosis (fig.4(d))

which is similar to the original wrinkling state (fig.4(a)). However, it is noted that the number

of wrinkles in this phase is generally less than that of original wrinkles, which is due to the fact

that some wrinkles are flattened or merged during the formation, growth and rearrangement of

ridges. To distinguish the wrinkling state before and after the ridge formation phase, the later

one is defined as "second wrinkling". The process of wrinkling to ridge and back to second

wrinkling is more notable with $\lambda_0 = 1.7$ than $\lambda_0 = 1.53$, as the compressive strain range is

about $\varepsilon_{w2} - \varepsilon_{w \to r} \approx 0.2$ with $\lambda_0 = 1.7$. Eventually the sencond wrinkling also evolves into

periodic doubling morphosis at $\varepsilon_{pd} = 0.48$ (fig.4(e)).

The morphology evolution under increasing overall compression with $\lambda_0 = 1.55 \sim 1.9$ is

similar with above process with $\lambda_0 = 1.7$, and the detailed results and corresponding critical
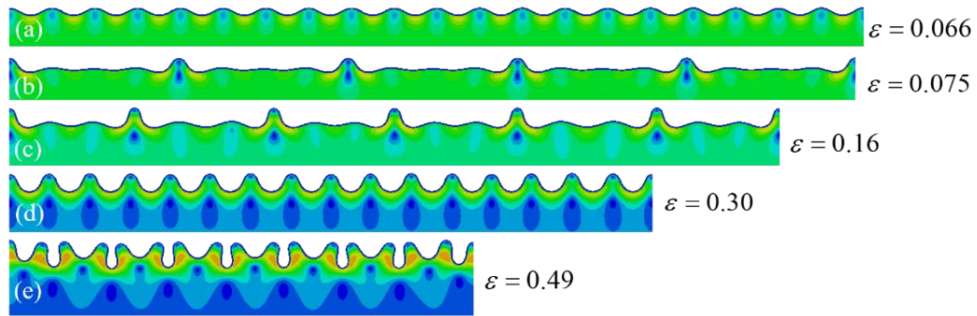
strains will be present in Section 2.3.

Fig. 4: Wrinkling to periodic ridge formation in an elastic bilayer system with a prestretch
$\lambda_0 = 1.7$. $\varepsilon_w = 0.0096, \varepsilon_{w \to r} = 0.068, \varepsilon_{w2} = 0.26, \varepsilon_{pd} = 0.48$. (a)wrinkling state(20
wrinkles); (b)initial periodic ridge formation; (c)subsequent ridge formation and self aligning;
(d)second wrinkling(16 wrinkles); (e)period doubling.

(3) $2.0 \le \lambda_0 \le 2.1$: Transition from wrinkling to disordered ridge formation, then to second

wrinkling and finally to period doubling. Ridges form when the overall compression reaches a

certain strain $\varepsilon_{w \to r} = 0.042$ (fig.5(b)(f)). But unlike (2), the formation of the initial ridges is less

periodical and the space between initial ridges are less regular. With increasing compression, there are formation and self aligning of new ridges (fig.5(c)). At $\varepsilon_{w2} = 0.35$, new ridges no longer form and the self aligning process has been completed, the surface enters the second wrinkling phase(fig.5(d)). The number of wrinkles in second wrinkling phase is almost reduced to half of that in original wrinkling phase. Finally, the system enters the period doubling phase (fig.5(e)).
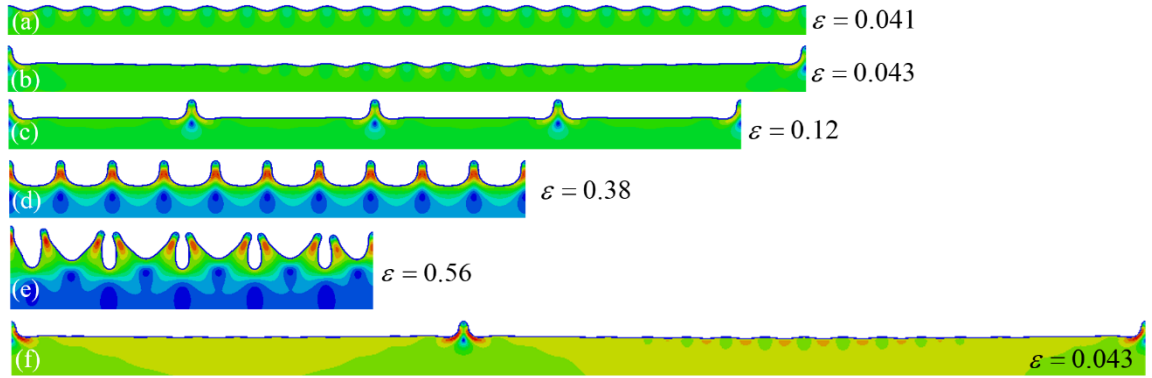

Fig. 5: Wrinkling to ridge formation in an elastic bilayer system with a prestretch $\lambda_0 = 2.0$. $\varepsilon_w = 0.0114$, $\varepsilon_{w \to r} = 0.042$, $\varepsilon_{w2} = 0.35$, $\varepsilon_{pd} = 0.55$. (a)wrinkling state; (b)initial ridge formation with $L = 20l_w$; (c)subsequent ridge formation and self aligning; (d)second wrinkling; (e)period doubling; (f)initial disordered ridges with $L = 30l_w$.

2.3 A surface morphology phase diagram

Combining the results of pre-stretch from $\lambda_0 = 1.1$ to $\lambda_0 = 2.1$, the surface morphology of the bi-layer system under different overall compression strains is presented in a phase diagram (fig.5). According to the classification in section 2.2, the phase diagram consists of five regions: base state (the flat surface), original wrinkling state (W1), Ridge formation state (RF), second wrinkling state (W2) and period doubling state (PD).
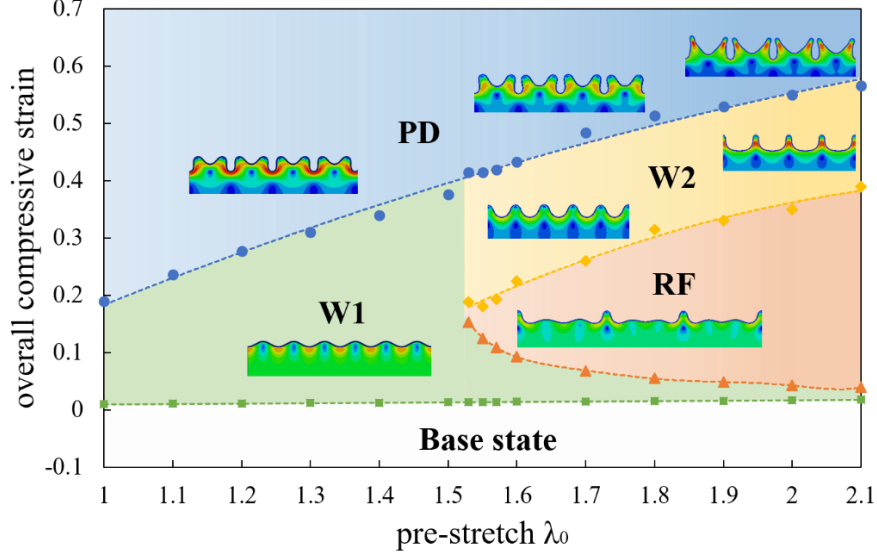
Fig. 6: A surface morphology phase diagram for a hyperelastic bilayer system ($\mu_f/\mu_s = 774$).

Ridge formation occurs when the pre-stretch is sufficiently large, roughly greater than 1.52 for the modulus ratio considered here ($\mu_f / \mu_s = 774$). It is possible that this critical pre-stretch depends on the modulus ratio. For the cases with large pre-stretches (>1.52), initial ridge formation occurs at a critical compressive strain $\varepsilon_{w \to r}$ that decreases with the increasing pre-stretch λ_0. In this case, multiple ridges form simultaneously, and the spacing between adjacent initial ridges increases with the increasing pre-stretch, as shown in fig.7. The initial ridge formation period is about $L_r = 2l_w$ with pre-stretch of 1.53, $L_r = 3l_w$ with pre-stretch of 1.55, 1.57, and 1.6; $L_r = 4l_w$ with pre-stretch of 1.7; $L_r = 5l_w$ with pre-stretch of 1.8 and 1.9. As the spacing increases, the interactions between the ridges weaken, and the ridge spacing becomes less regular and periodic, as shown in the case of pre-stretch of 2.0 in fig.7(e).
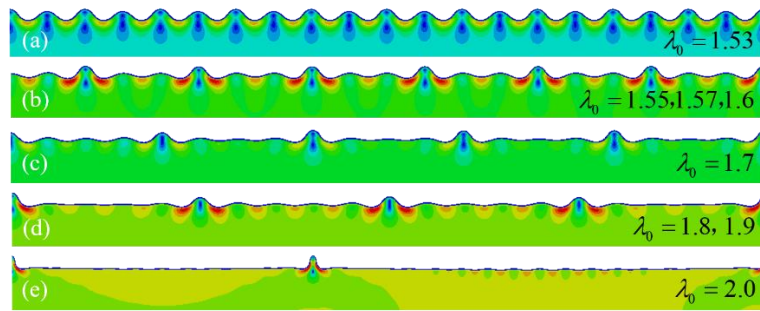

Fig.7 initial ridge formation with pre-stretch from 1.55 to 2.0

After the initial ridge formation (periodic or not), additional ridges may form between the initial ridges as the applied compressive strain increases, reducing the spacing between adjacent ridges. With increasing compression, ridge formation state ends up with second wrinkling state at a critical compressive strain ε_{w2} that increases with the increasing pre-stretch λ_0. The process between initial ridge formation ($\varepsilon_{w \to r}$) and second wrinkling (ε_{w2}) is longer with larger pre-stretch. As the pre-stretch decreases to some where between 1.52 and 1.53, two phase boundaries get closer and finally converge to a single point.

With increasing compression, the wrinkling, both original wrinkling and second wrinkling, transition in to period doubling. The critical strain ε_{pd} shows positive correlation with pre-stretch, which is consistent with the result of previous researchers.

The reasons behind the phenomenon of periodic ridge formation and the positive correlation between ridge periodicity and pre-stretch will be discussed further in Section 3.

3. Mechanism of the initial periodic ridge formation

3.1 Static force method with different model size

For the bi-layer systems, there exists a critical substrate pre-stretch λ_{r1}, below which the surface morphology of the system experiences transition from wrinkling to periodic doubling under increasing overall compression; while beyond which, the surface morphology first changes from wrinkling to ridges and subsequently forms periodic doubling folding. The pre-stretch plays an important role in the evolution process of the system surface topography, because it leads to the change of mechanical properties of the bi-layer neo-Hookean material. The pseudo-dynamic method is a relatively direct way to simulate the morphology evolution process of the bi-layer systems, and it just presents the phenomena. In order to understand and reveal the role pre-stretch plays in the morphology evolution process, the "static force method" will be used to quantitatively study the effect of pre-stretch on the mechanical properties of the bi-layer system.

The periodicity of ridge formation in Section 2 indicates that a model of length of the

ridge formation period $L = nl_w$ in combination with periodic boundary conditions can be used to simulate and represent a system of infinite number of wrinkles, thus the computational cost is reduced. The selection of model size, or the model length can refer to the results of pseudo-dynamic method, which will be discussed in more detail later.

The specific approach of static-force method is illustrated in the figure x. The first step is to introduce the initial imperfection into the bi-layer system. The imperfection is the shape of the first mode, the sinusoidal wrinkle, with amplitude $\Delta_{imp} = 1/50 h_f$, phased such that the left and right edges of the surface are the wrinkle peaks. The next step is the pre-stretch of the substrate, which can be done by the Abaqus "model change" function. Then the system is subjected to overall compression, during this step the model boundary conditions are the same with the pseudo-dynamic method. On the left and right vertical edges, the shear tractions are zero and a prescribed uniform horizontal displacement is imposed to create the overall compression; On the bottom edge, the shear tractions and the vertical displacement are zero. After the overall compression, the left and right vertical edge maintain the prescribed uniform horizontal displacement and zero shear traction, and an additional vertical displacement Δ is then imposed on the wrinkle peak at the left and right edges to propel the system towards an e periodic ridge formation. In this way, the ridge solution obtained here correspond to a periodic ridge mode with period $L = nl_w$. The other parameters of the model are the same with Section 2.1.
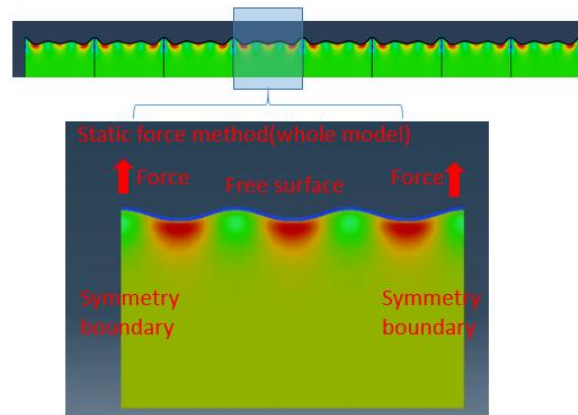

Fig.8 Schematic for static force method.

3.2 Effect of pre-stretching and overall compression on nonlinearity of bi-layer system force-displacement behavior

The pre-stretch plays a key role in controlling the surface morphology evolution process by affecting the mechanical property of the bi-layer neo-Hookean system. According to the results of pseudo-dynamic method, the critical pre-stretch λ_r is between 1.52 and 1.53, thus

we first investigate the mechanical behavior of the bilayer around the critical pre-stretch λ_r

to see what happens in the overall compression process. We will present three typical cases of

pre-stretch $\lambda_0 = 1.52$, 1.53 and 1.55 in this section. By the results from pseudo-dynamic

method, the initial ridge formation period is about $2l_w$ and $3l_w$ for $\lambda_0 = 1.53$ and 1.55,

respectively, thus the model size $L = 2l_w$ and $L = 3l_w$ are selected for $\lambda_0 = 1.53$ and 1.55

respectively in static-force method. As no ridges will form at pre-stretch of 1.52, the model size

can be arbitrary. However, two model sizes of $L = 2l_w$ and $L = 3l_w$ are selected for $\lambda_0 = 1.52$

to make comparison with the other two cases.

At a sequence of fixed overall compressive strain $\varepsilon_w < \varepsilon < \varepsilon_{pd}$, additional vertical

displacement Δ is imposed at wrinkle peaks of two edges. The associated reaction force F

is plotted as a function of the normalized imposed vertical displacement Δ / h_f (fig.9, fig.10(a)

and fid.11(a)). Along with the force-displacement curves, the strain energy difference

$U_{diff} = U - U_w$ between the wrinkling state and the ridge state is also plotted against the

normalized imposed vertical displacement Δ / h_f (fig.11(b)). The energy relationship when

vertical displacement Δ is imposed to the elastic system can be written as

$$d(U_{diff}) = Fd\Delta \tag{2}$$

The reaction force F represents the tangent slope of the strain energy difference curve. Those

equilibrium solutions with $F = 0$ in the force-displacement curve corresponds to the

stationary points in the strain energy difference curve. If the equilibrium solution refers to a

local minimum point of energy, i.e. $dF / d\Delta > 0$, then it is a stable equilibrium state; on the

contrary it will be unstable.

Besides, Fig.10(b) and Fig.11(c) present the trajectory plot of all the equilibrium solutions at different compression level. The ordinate $V - V_0$ reflects the formation and growth of wrinkles and ridges, where V is the vertical displacement of the wrinkle peaks' at both edges of the model corresponding to the $F = 0$ equilibrium state, and V_0 is the vertical displacement of the upper surface of the perfection-free model. For comparison, the results by pseudo-dynamic method in Section 2 is also presented.
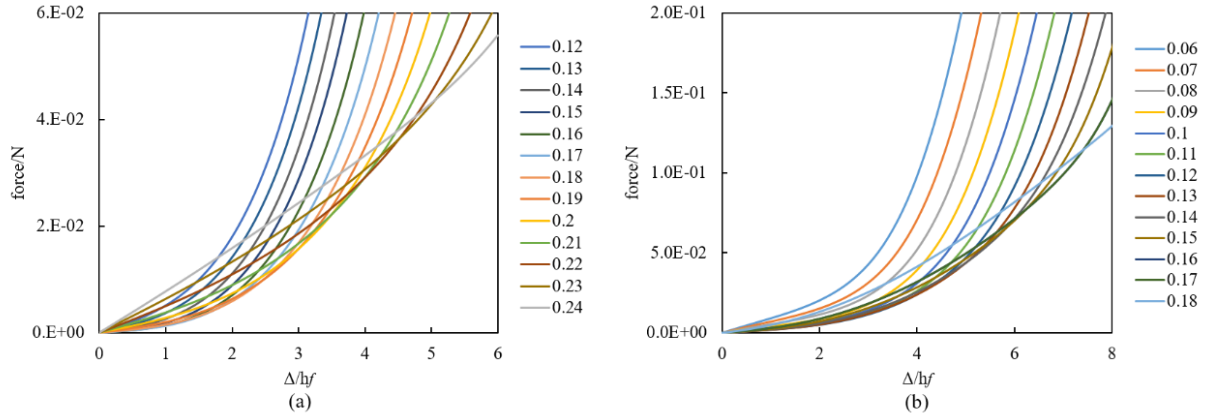
(1) $\lambda_0 = 1.52$.

Fig. 9: reaction force-displacement curves at various overall compressive strain with pre-stretch $\lambda_0 = 1.52$: (a) model size $L = 2l_w$; (b) model size $L = 3l_w$.

For model size $L = 2l_w$ (fig.9(a)) and $L = 3l_w$ (fig.9(b)), at each compression level in the diagram, the reaction force increases monotonically with the displacement, and there is only one equilibrium solution at $F = 0$, the solution of wrinkling state with $\Delta = 0$. The results mean during the overall compression, spontaneous ridge formation with a period of $L = 2l_w$ or $L = 3l_w$ is impossible. To verify the possibility of ridge formation with other periods, the same operation was performed for models of other sizes, and the results were quite consistent with Fig.9(a) and (b). From static-force method, it can be concluded that with pre-stretch=1.52, during the overall compression, ridges cannot spontaneously form without the external pulling force, which is consistent with the conclusion by pseudo-dynamic method. Since ridges do not

form, the system will remain in the wrinkling state until it reaches the critical strain ε_{pd}, and then will undergo the wrinkling to period doubling transition.

By detailed analysis of fig.9(a) and (b), it is found with the given pre-stretch=1.52, the overall compression shows softening-hardening effect on the ridge promotion process. There exists a compressive strain, before which the increase of overall compression has a softening effect on the force-displacement curve, as the initial slope of the curve decreases; and beyond which the increase of compression hardens the force-displacement curve, as the initial slope of the curve increases and the curves shifts upwards.
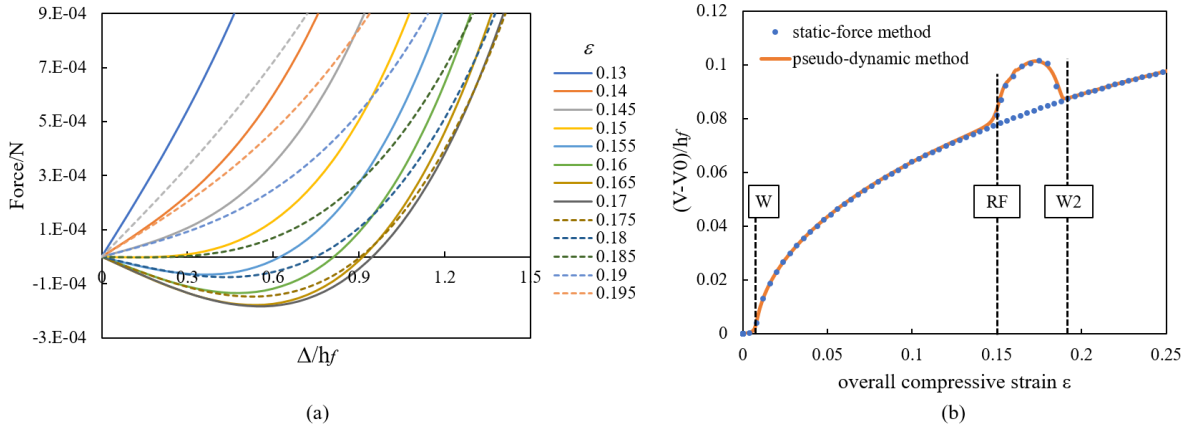
(2) $\lambda_0 = 1.53$.

Fig. 10: Pre-stretch $\lambda_0 = 1.53$ with model size $L = 2l_w$: (a) reaction force-displacement curves at various overall compressive strain; (b) the equilibrium solutions trajectory by static-force method and pseudo-dynamic method.

With pre-stretch=1.53, the overall compression also shows softening-hardening effect on the force-displacement curves. The softening process is represented by solid lines in fig.10(a) while hardening process by dashed lines. In the range of $\varepsilon < 0.17$, the increase of overall compression softens the force-displacement curve, causing the initial slope decreased. In the softening process, there exists a critical strain $\varepsilon_{w \to r} \approx 0.15$, beyond which the initial slope changes from positive to negative and a second equilibrium solution of $F = 0$, except the wrinkling solution with $\Delta = 0$, occurs. This new equilibrium solution with $dF / d\Delta > 0$ refers

to a stable ridge. The occurrence of ridge solution corresponds to the wrinkling to ridge transition, as illustrated in fig.10(b). As the compression increasing, the ridge solution moves from zero to the right, meaning that the ridge height increases to the maximum.

In the range of $\varepsilon > 0.17$, the increase of compression hardens the force-displacement curve, causing the initial slope increased and the stable ridge solution moving left. During the re-hardening process, there exists another critical strain $\varepsilon_{w2} \approx 0.185$, beyond which the initial slope regains positive, and the ridge solution vanishes. The vanishment of ridge solution corresponds to the ridge to second wrinkling transition. Fig.10(b) shows that the critical strain $\varepsilon_{w \to r}$ and ε_{w2}, and the ridge growing height from two simulation methods coincide very well.
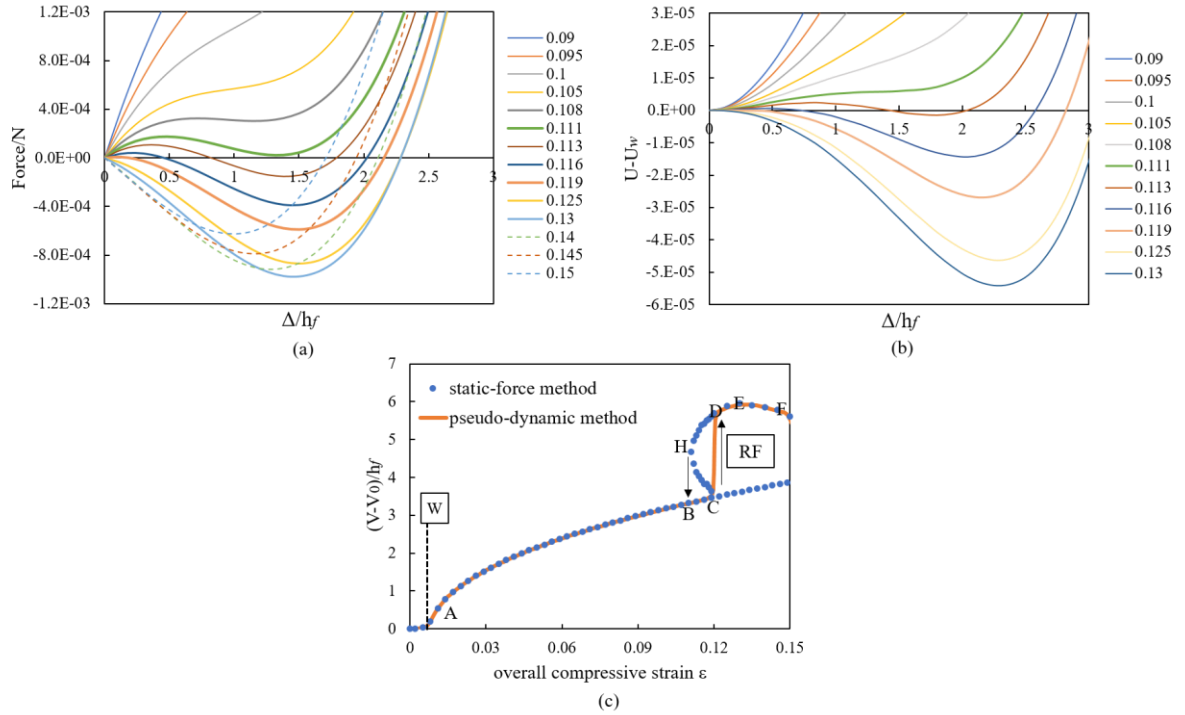
(3) $\lambda_0 = 1.55$.

Fig. 11: Pre-stretch $\lambda_0 = 1.55$ with model size $L = 3l_w$: (a) reaction force-displacement curves at various overall compressive strain; (b)energy difference-displacement curves; (c) the equilibrium solutions trajectory by static-force method and pseudo-dynamic method.

With pre-stretch=1.55, the overall compression also shows softening-hardening effect on

the force-displacement curves. The softening process is represented by solid lines in fig.11(a) while hardening process by dashed lines. Two critical compressive strain, $\varepsilon_{w \to r} \approx 0.111$ and $\varepsilon_{r \to w} \approx 0.119$, are determined, and the mechanical behavior of the system can be characterized by the following three stages:

Stage1: $\varepsilon_w < \varepsilon < \varepsilon_{r \to w}$. With the increase of overall compression, the force-displacement curve is softened, the initial slope continues to decrease, and the curve becomes non-monotonous. There is only one equilibrium solution of $F = 0$, which is the wrinkling state. When the strain reaches $\varepsilon_{r \to w} = 0.111$, the second equilibrium solution of $F = 0$ with non-zero Δ appears. This stage is represented by segment AB in Fig.11(c);

Stage2: $\varepsilon_{r \to w} < \varepsilon < \varepsilon_{w \to r}$. As the compression increases, the force-displacement curve is further softened, and the curve produces three equilibrium solution of $F = 0$: (a) the first solution with $\Delta = 0$ and $dF/d\Delta > 0$ refers to stable wrinkling state, corresponding to the local minimum point of energy ; (b) the second solution with small Δ and $dF/d\Delta < 0$ refers to an unstable ridge solution, corresponding to the local maximum point of energy; (c) the third solution with large Δ and $dF/d\Delta > 0$ refers to a stable ridge solution, corresponding to the local minimum point of energy. When compression reaches $\varepsilon_{w \to r}$, the second ridge solution vanishes.

The first wrinkling and the third ridge solutions are both stable, but there exists a Maxwell strain, $\varepsilon_{r \to w} < \varepsilon_{\mathrm{maxwell}} < \varepsilon_{w \to r}$, at which the elastic potential energy of two solutions are equal. From fig.11(b), in the range of $\varepsilon_{r \to w} < \varepsilon < \varepsilon_{\mathrm{maxwell}}$, the third ridge solution has higher energy than the wrinkling state, thus it is a metastable solution; while in the range of $\varepsilon_{\mathrm{maxwell}} < \varepsilon < \varepsilon_{w \to r}$, wrinkling becomes metastable solution.

Although the third ridge solution is stable and maybe lower-energy, snapping from the wrinkling state to the third state requires overcoming the energy barrier caused by the second ridge solution. Thus, in **stage 2,** with increasing compression, the system maintains the wrinkling state until $\varepsilon_{w \to r}$. This process is represented by segment BC in fig.11(c). Similarly,

if the system has already formed stable ridges, then in the releasing process, the system will not snap from the ridge state back to the wrinkling state until compression released to $\varepsilon_{r \to w}$, because the ridge to wrinkling transition also has to overcome the energy barrier caused by the second ridge state. Thus, in **stage 2**, with decreasing compression, the system will maintain the ridge state. This process is represented by segment DH in fig.11(c). The difference in surface morphology evolution during compression and releasing process in this stage contributes to the hysteresis effect shown as BCDH in Fig.11(c).

Stage 3: $\varepsilon \geq \varepsilon_{w \to r}$. In this stage, the equilibrium solutions of $F = 0$ are reduced to two points: (a) the first solution with $\Delta = 0$ and $dF / d\Delta < 0$ refers to the unstable wrinkling state, corresponding to the local maximum point of energy; (b) the second solution with nonzero Δ and $dF / d\Delta > 0$ refers to stable ridge state, corresponding to the local minimum point of strain energy. When compression increases to $\varepsilon_{w \to r}$, the system immediately snaps from the higher-energy unstable wrinkling state to the lower-energy stable ridge state, and the ridge's height surges to the nonzero Δ. This snap-through behavior is represented by segment CD in fig.11(c).

After the snap-through, with the increasing compression, the ridge solution first moves to the right and then move back to the left, which is due to the re-hardening effect of overall compression. The reduction of $V - V_0$ by segment DEF in fig.11(c) also reflects that the ridge height is finite and the ridge cannot grow indefinitely. Fig.11(c) shows that the surface revolution results from two simulation methods coincide very well.

Combining the results of $\lambda_0 = 1.52$, 1.53 and 1.55, It could be summarized that in the early stages of overall compression, the compression softens the force-displacement curve of the system, and thus makes it easier to pull the wrinkling peak upwards to form a ridge; as the overall compression continuously increases, the force-displacement curve rehardens, thus pulling the wrinkling peak upward requires greater pulling force and external work. The soften-reharden effect caused by overall compression provides the possibility for multiple equilibrium solutions, thus provides the possibility for ridge formation. For $\lambda_0 = 1.52$, before re-hardening effect, the overall compression does not soften the system enough, thus the system does not

have a ridge equilibrium solution throughout the entire compression process. For $\lambda_0 = 1.53$, the softening effect is pronounced, thus ridge solution appears. But the compressive range between $\varepsilon_{w \to r} \approx 0.15$ and $\varepsilon_{w2} \approx 0.185$ is relatively small, thus the system turns back to wrinkling state very soon. For $\lambda_0 = 1.55$, the softening effect is more pronounced, and before the initial formed ridges turns back to original wrinkling state, new ridges form.

The degree, to which the system's force-displacement curve is softened, plays a key role in the spontaneous ridges formation process, and the parameter that controls the softest degree is the pre-stretch λ_0. In the case of $\lambda_0 = 1.52$, 1.53 and 1.55, larger pre-stretch leads to stronger softening effect. To investigate the influence of pre-stretch on the nonlinear force-displacement behavior, the static force method is applied at each compression stage with pre-stretch ranging from 1.5 to 2.0. The model used to generate the results in fig.12 are all of size $L = 3l_w$.
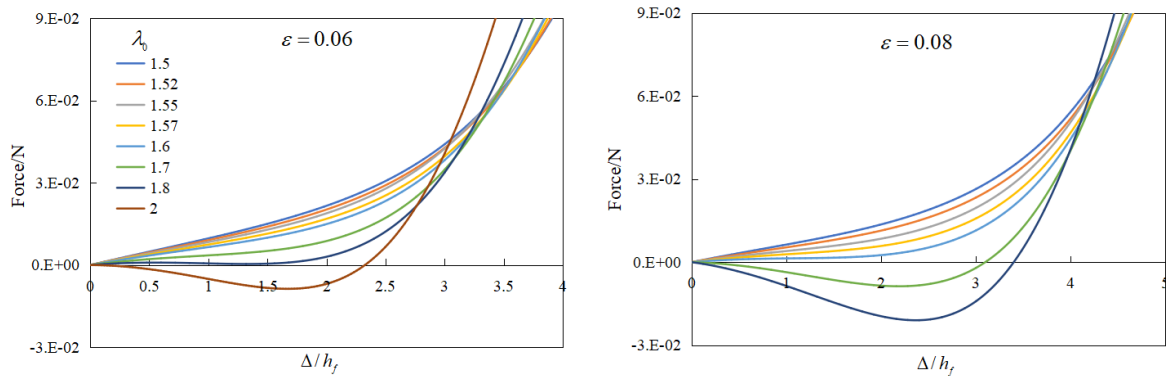

Fig.12 reaction force-displacement curves at the same overall compression strain with various pre-stretch.

The force-displacement curves show that with the same compressive strain level, the softening effect is more obvious with larger pre-stretch. This result is consistent with the conclusions of previous researchers (), that the pre-stretch produces softening for outward displacement which favors ridge formation. With larger pre-stretch, the system's force-displacement curve is softened to a larger degree, thus the wrinkling to ridge transition happens at a lower compressive strain level, which explains the result by pseudo-dynamic method that critical strain decreases with pre-stretch.

3.3 Initial ridge formation period

The previous section reveals that, it is the combination of the soften effect by pre-stretch and the soften-reharden effect by overall compression that determines whether the ridge will form spontaneously. If the pre-stretch of the substrate exceeds the critical value λ_r, the surface morphology of the system will spontaneously evolve from wrinkles to ridges when the overall compression reaches associated compressive strain critical value $\varepsilon_{w \to r}$. The results of the pseudo-dynamic method show that the initial arrangement of ridges between pre-stretch of 1.53 to 1.9 is highly ordered and periodic, and the ridge period shows a negative correlation with the pre-stretching of the substrate. To reveal the mechanism behind the ridge formation period, this section will apply the static-force method to investigate the nonlinear force-displacement behavior of the system with various ridge formation periods.

The pre-stretch investigated here is 1.55, 1.57, 1.6, 1.7, 1.8 and 2.0. For each pre-stretch of the substrate, the static-force method is applied on series of finite element model with the model size $L = nl_w$, where n starts from 2 to some integer n_{max}. The model size L actually represents the initial ridge formation period. $L = 2l_w$ represents refers the minimum possible period, that is, every other wrinkle, a ridge is formed. $L = n_{max}l_w$ represents the maximum possible period. The simulation result indicates that for each pre-stretch, there may be an upper limit $L = n_{max}l_w$ for the initial ridge formation period, and n_{max} may vary with the pre-stretch. The determination of n_{max} will be discussed later. It should be noted that except the model length L, any other parameter of the finite element model with the fixed pre-stretch are completely the same, such as the dimensions in the thickness direction and the mesh density.

Fig.13 presents the force-displacement curves with $\lambda_0 = 1.6$ at various compression level. The model sizes considered here are $L = 2l_w$ to $L = 5l_w$. In this model size range, when the overall compression increases to a certain level, the initial slope of the force-displacement curves changes from positive to negative, leaving the wrinkling state an unstable equilibrium state. The tendency in the plot of $L = 3l_w$, $4l_w$, and $5l_w$ is consistent with the three stages of

$\lambda_0 = 1.55$ with $L = 3l_w$, as summarized in Section 3.2. However, with model size $L = 2l_w$, the force-displacement curve is more similar to the result of $\lambda_0 = 1.53$ as shown in fig.10(a), evolving directly from stage 1 with one equilibrium solution (stable wrinkling) to stage 3 with two equilibrium solution (unstable wrinkling and stable ridge). As there is no stage 2, where the curve produces three equilibrium solution of $F = 0$, there is either no energy barrier caused by the medium equilibrium solution (the unstable ridge), thus between compression and release no hysteresis exists with ridge period $L = 2l_w$. In this case, $\varepsilon_{w \to r} = \varepsilon_{r \to w}$, and the ridge height increases continuously during the ridge formation process, similar with fig.10(b).
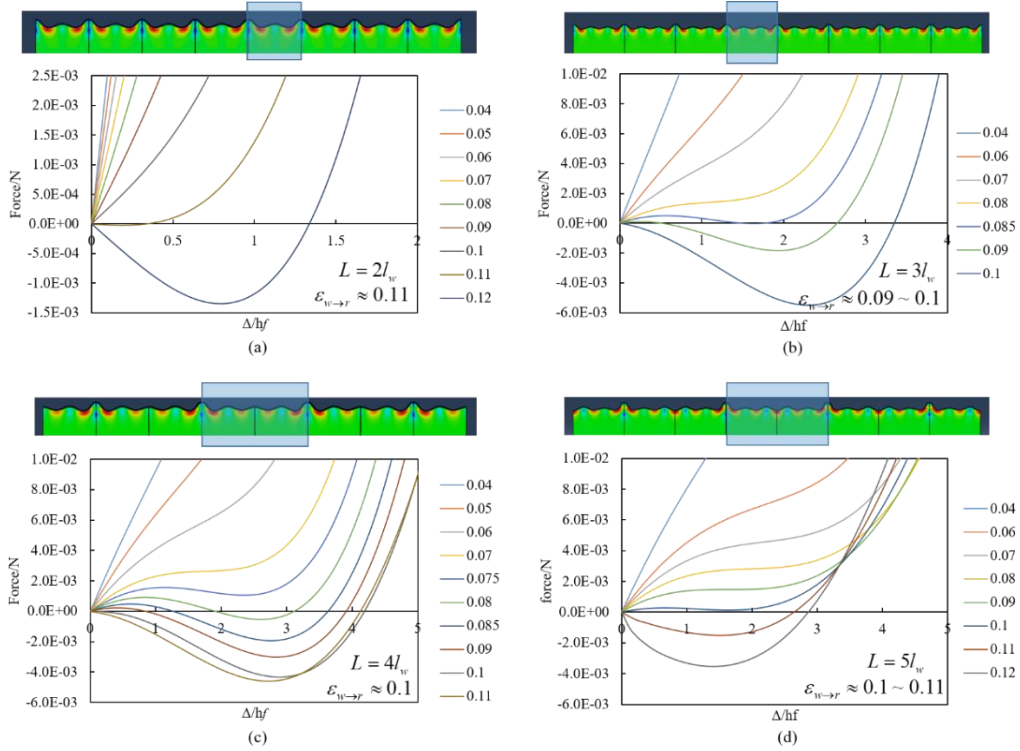

Fig. 13: Reaction force-displacement curves at various overall compressive strain with pre-stretch $\lambda_0 = 1.6$: (a) model size $L = 2l_w$; (b) model size $L = 3l_w$; (c) model size $L = 4l_w$; (d)model size $L = 5l_w$.

When the ridge formation period takes $L = 6l_w$, the model is firstly subjected to overall compression $\varepsilon = 0.09$ (fig.6 state O), then the overall compression is kept unchanged, and upward displacements are imposed at the wrinkle peaks 1 and 7 (fig.6) to induce ridge

formation at these two locations. The result is surprising. With the increase of imposed Δ, not only the height of peaks 1 and 7 increase (solid blue line), but the height of peak 4 in the middle of the model also increases spontaneously (dashed blue line), indicating a third ridge is forming. When the imposed Δ reaches state A and state B, the reaction forces at peaks 1 ,4 and 7 are all 0, and the ridge heights of these three positions are exactly the same. The equilibrium ridge solution is unstable at state A, while is stable at state B. New ridge forming at peak 4, this phenomenon implies that: firstly, because between two ridges separated by five wrinkles a new ridge will spontaneously form, the ridges period of $L = 6l_w$ is unstable, thus is unpractical.

Since $L = 6l_w$ is already proved to be an impossible ridge period, then a larger ridge period is naturally impossible; Secondly, the formation and growth of ridge at peak 1 and 7 will promote the formation of ridge at peak 4, which reflects the synergy of initial ridge formation. However, if the imposed Δ increases further (such as fig.6 state C), the height of peak 4 will begin to decrease. This is because the material is incompressible, and the left, right and bottom boundary of the system are kept unable immobile, so under the condition of plane strain, the continuous growth of the ridge requires a reduction in the height of the adjacent peaks at the expense. Therefore, in the process of continuing ridge growth, ridges also show competition among others.
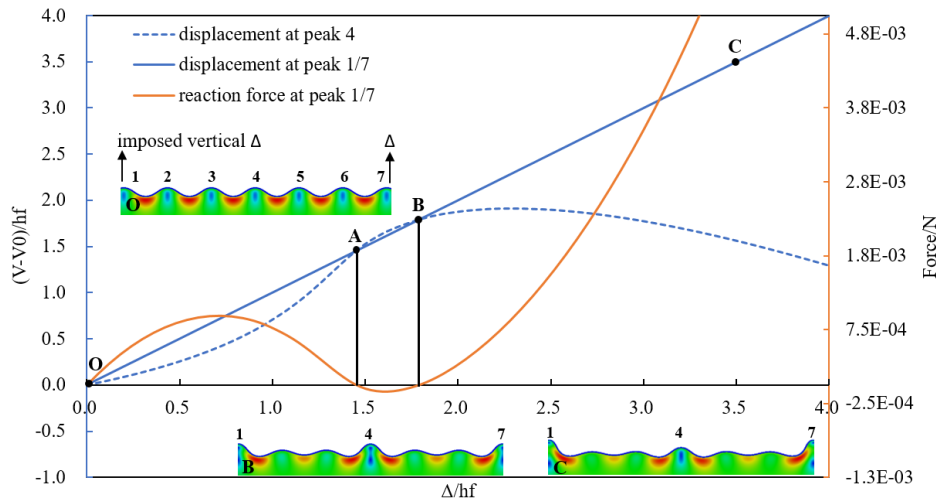

Fig.14 ridge height-displacement curves and reaction force-displacement curve with pre-stretch $\lambda_0 = 1.6$ and model size $L = 6l_w$.

All in all, according to the result of static force method, with substrate pre-stretch $\lambda_0 = 1.6$, although the evolutionary process is somehow slightly different within ridge period from $L = 2l_w$ to $L = 5l_w$, the ridge formation is all possible to happen. The critical compressive strain $\varepsilon_{w \to r}$ can be determined by the force-displacement curve's initial slope transitioning from positive to negative. It is found that $\varepsilon_{w \to r}$ varies slightly with the ridge formation period L. As the period increases, $\varepsilon_{w \to r}$ firstly decreases and then increases. There exists a minimum critical compressive strain, $\varepsilon_{w \to r} \approx 0.095$, which coincides with the critical strain 0.096 obtained by pseudo-dynamic method very well. The minimum $\varepsilon_{w \to r}$ corresponds to ridge period of $L = 3l_w$, which is also consistent with the actual period appearing in pseudo-dynamic method. This coincidence suggests that periodic ridges with different period may all have the potential to form, but the most likely period of ridge formation should be the one corresponding to the lowest critical strain.

The results under other pre-stretches also support this hypothesis (fig.13). Under each pre-stretch λ_0, there is a possible ridge formation period range, from $L = n_{min}l_w$ to $L = n_{max}l_w$. In this range, periodic ridge formation with either period is possible. For all pre-stretch, $n_{min} = 2$, but n_{max} increases with pre-stretch. Under each λ_0, the critical compressive strain $\varepsilon_{w \to r}$ firstly decreases and then increases with L, thus there is a minimum $\varepsilon_{w \to r,min}$ for each λ_0. By comparison with fig.5, it is found $\varepsilon_{w \to r,min}$ for each λ_0 coincides very well with the critical strain by pseudo-dynamic method. Besides, the period L corresponding to $\varepsilon_{w \to r,min}$ under each pre-stretch, except $\lambda_0 = 2$, also coincides exactly with the result by pseudo-dynamic method.
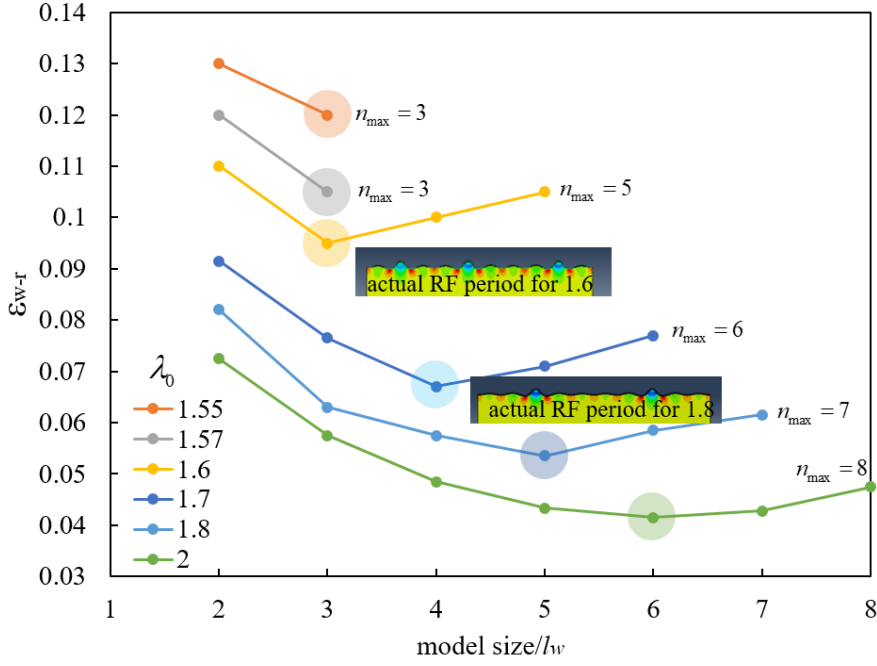
Fig. 15: the relationship between critical overall compressive strain $\varepsilon_{w \to r}$ and model size

$$L = n l_w \text{ with pre-stretch } \lambda_0 = 1.55 \sim 2.0 .$$

To help to explain this result, we plot the equilibrium solution trajectory from different ridge formation period in the same plot. Take the case under $\lambda_0 = 1.6$ and $\lambda_0 = 1.8$ as demonstrations (fig.8). In the actual experiment or the previous pseudo-dynamic method, the overall compressive strain ε is continuously increased from zero to a certain level. When ε increases to the smallest critical compressive strain $\varepsilon_{w \to r, \min}$ capable for forming ridges, the system, subjected to a slight perturbation, immediately and spontaneously jumps to the ridge state with corresponding ridge period—that is, the initial bridge begins to form.
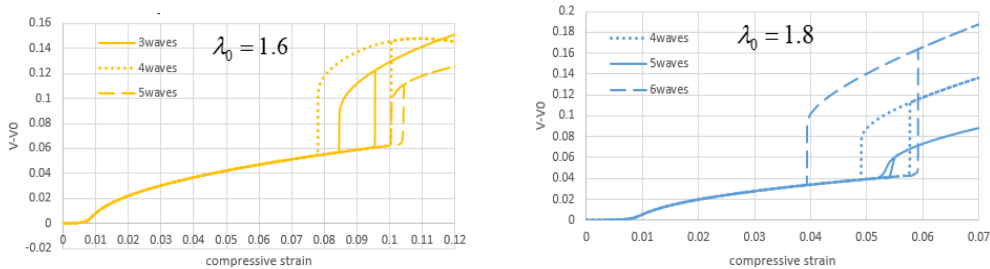

Fig.16

For the pre-stretch $\lambda_{r1} < \lambda_0 < \lambda_{r2}$, The results from static force method and the pseudo-dynamic method, both the critical compressive strain and the ridge formation period, coincides well with each other. If the result from static force method also applies to the case for $\lambda_0 > \lambda_{r2}$, it will be reasonable to extrapolate that under $\lambda_0 = 2$, periodic ridges should form spontaneously at $\varepsilon_{w\to r,\min} \approx 0.42$ with corresponding ridge period $L = 6l_w$. However, there is obvious discrepancy between the result of two methods. By pseudo-dynamic method, the initial formation of the ridge is disordered and not well periodical, and the space between ridges is neither 5 or 6 wrinkles, which are the most likely ridge periods suggested by the static-force method. There must therefore be some other factors that make the conclusion applicable to $\lambda_{r1} < \lambda_0 < \lambda_{r2}$ no longer reasonable to $\lambda_0 > \lambda_{r2}$.

It should be pointed out that in the static-force method, in order to reduce the cost of computation, the periodic boundary condition is introduced in the bi-layer system with various ridge formation period, thus the above results by the static-force method is actually based on the assumption that the formation and growth of all ridges are completely consistent and synchronized. As mentioned before in Section 3.3, in the example of $\lambda_0 = 1.6$ with ridge period $L = 6l_w$, a ridge may promote the formation of another ridge during its early formation stage, but the continued growth of the ridge is at the expense of the reduction of the crest of the adjacent part, so that when the ridge grows to a certain height, it may in turn inhibit the growth of the ridges nearby. The relationship between the ridges develops from the initial synergy to later competitive or trading-off stage, which indicates the assumption in the previous static-force method that the formation and growth of all ridges are completely consistent and synchronized may only apply to the mutually synergistic stage of ridge formation, and no longer apply to the trading-off stage. The detailed discussion for the disordered ridge formation will be presented in the next section.

3.4 Formation of periodic ridges and disordered ridges

Since the amplitude of the initial sinusoidal imperfection is unchanged in the surface, the wrinkles produced subsequently also have translational symmetry in the surface. In the critical state that initial ridges are about to arise, every wrinkle should have the same potential to transition into a ridge due to this translational symmetry. But the formation and growth of a ridge is at the expense of decrease in the height of the wrinkle peaks nearby, so in reality the

wrinkles trade off with each other, and in the end only some of the wrinkles can jump into ridges, while the others will be flattened. The equidistant periodic arrangement of ridges is the result of the configuration force caused by the translational symmetry of the wrinkling surface. Similarly, the rearrangement of ridges during subsequent ridge formation is also the result of the configuration forces under translational symmetry. Theoretically speaking, if the wrinkling state has perfect translational symmetry, then the formation of the initial periodic ridges should be perfectly synchronized and consistent. However, in the pseudo-dynamic simulation or actual experimental process, it is impossible to ensure the perfection of translational symmetry, there will always be more or less non-translational symmetry perturbation, such as the interference of boundary conditions. The wrinkle to ridge transition is an unstable process--that wrinkles will snap dynamically to ridges. In this dynamic snapping process, the non-translational symmetry perturbation would cause some of the ridges that should have been formed synchronously to transition faster than others, and this asynchrony of ridge snapping may lead to the disordered initial ridge arrangement.

The above analysis should apply to the situation with pre-stretches $\lambda_{r2} > \lambda_0 > \lambda_{r1}$ and $\lambda_0 \geq \lambda_{r2}$, but periodic ridges form in the former case and disordered ridges form in the latter case. This difference suggests that the pre-stretch affects the sensitivity to perturbations during the periodic ridge formation process. In the case of $\lambda_{r1} < \lambda_0 < \lambda_{r2}$, the sensitivity to perturbation is lower, the initial ridges are almost synchronized and thus periodic arranged. But under pre-stretch $\lambda_0 > \lambda_{r2}$ the wrinkle-snapping-to-ridge process is more sensitive to perturbations.

To verify the hypothesis, the pseudo-dynamic method is applied again with damping factor $\beta = 0.0002, 0.0005$ for the case of pre-stretch $\lambda_0 = 1.7, 1.8, 2.0$. The other model parameters are the same with Section 2.1. The artificial damping is a computational ploy that stabilize the unstable transition from wrinkles to ridges, allowing the computation to pass through the snapping process, and can adjust the degree to which perturbation affects the snapping process. The focus here in on the initial ridge formation, thus the detailed formation and grow process of the initial ridges for $\lambda_0 = 1.7, 1.8, 2.0$ is presented in fig.15~17.
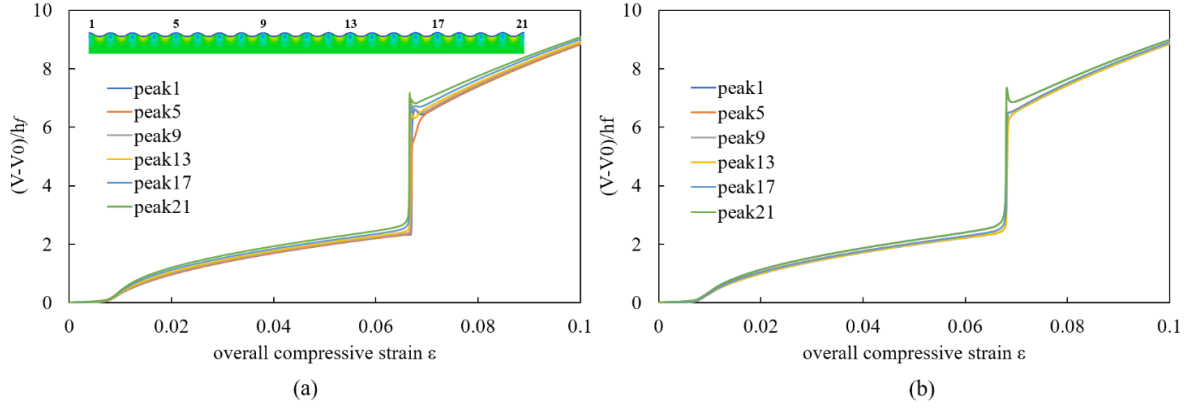
Fig.15 ridge formation and growth process with $\lambda_0 = 1.7$, (a) damping factor $\beta = 0.0002$; (b)

$$\beta = 0.0005.$$

For the case of a pre-stretch of 1.7, whether the damping factor takes 0.0002 or 0.0005, the height of the 1st, 5th, 9th, 13th, 17th, and 21st wrinkles increases dramatically when the critical strain $\varepsilon_{w \to r}$ is reached, transitioning almost synchronously to become ridges, and the ridges period when the initial ridges are formed is consistent with the results in section 3.3.
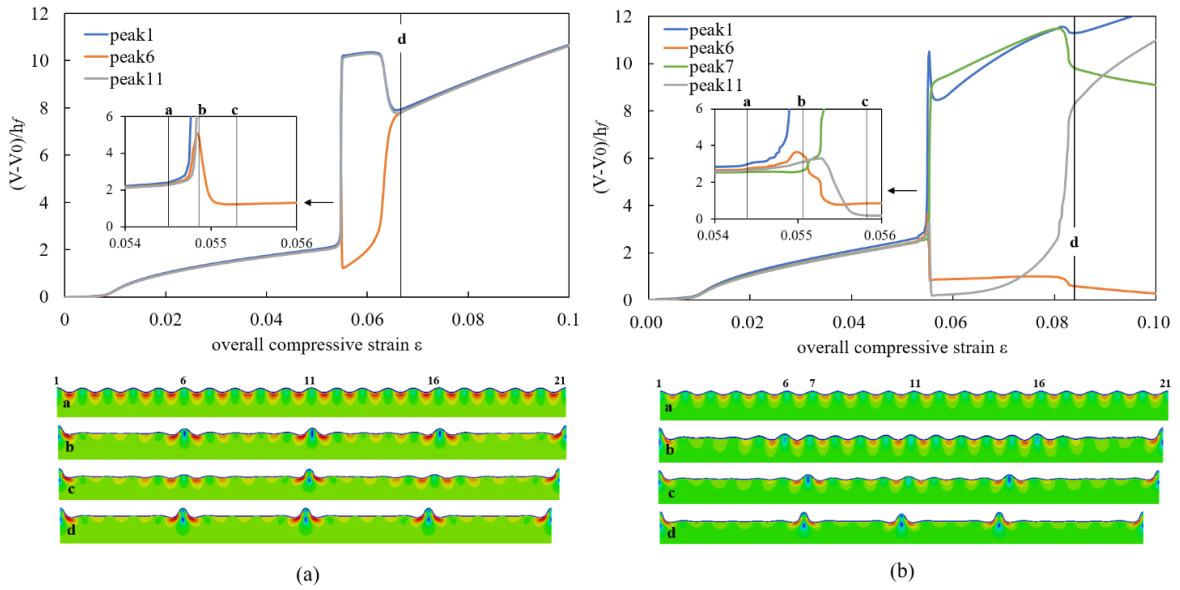

Fig.16 ridge formation and growth process with $\lambda_0 = 1.8$, (a)damping factor $\beta = 0.0002$; (b) β

$$= 0.0005.$$

For the case of pre-stretch of 1.8, when the damping is 0.0002, the ridges formation goes through several stages from stage a to stage d. In stage b, the 1st, 6th, 11th, 16th and 21st

wrinkles, spaced by three other wrinkles, all arise to become the potential initial ridges. The period of potential initial ridges is consistent with the result $L = 4l_w$ in fig.16. It is noted that the 1st, 11th and 21st wrinkles are more predominant than the other two wrinkles. Immediately after stage b, the height of the 3 dominant wrinkles continued to increase, while the other 2 potential wrinkles are reduced. At stage c the wrinkle-snapping-to-ridge process is completed. It is noted that at stage c, the positions 6th and the 16th remain the wrinkle state, while the other position has been flattened and almost lost the morphosis of wrinkling. When compression increases further, the wrinkles at 6th and 16th positions snap to ridges, and the 5 ridges automatically trade off to the same height during this dynamic process, reaching the state d in the fig.16(a). Finally, these 5 initial formed ridges grow with the stable period $L = 4l_w$ until the subsequent new ridges arise.

When the damping factor is 0.0005, the ridge formation process is significantly different with the case of damping 0.0002. The ridge formation also goes through several stages from stage a to stage c, as illustrated in fig.16(b). At stage b, the 1st, 6th, 11th, 16th and 21st wrinkles all arise to become the potential initial ridges. But the 1st and 21st wrinkles are more predominant than the other 3 wrinkles. In the process of these 2 dominant wrinkles snapping, the 6th, 11th and 16th wrinkles are flattened, and the nearby 7th and 10th wrinkles becomes predominant. Finally at stage c, the 1st, 7th, 10th and the 21st wrinkles complete the transition to ridges, and the ridge period is no longer constant.
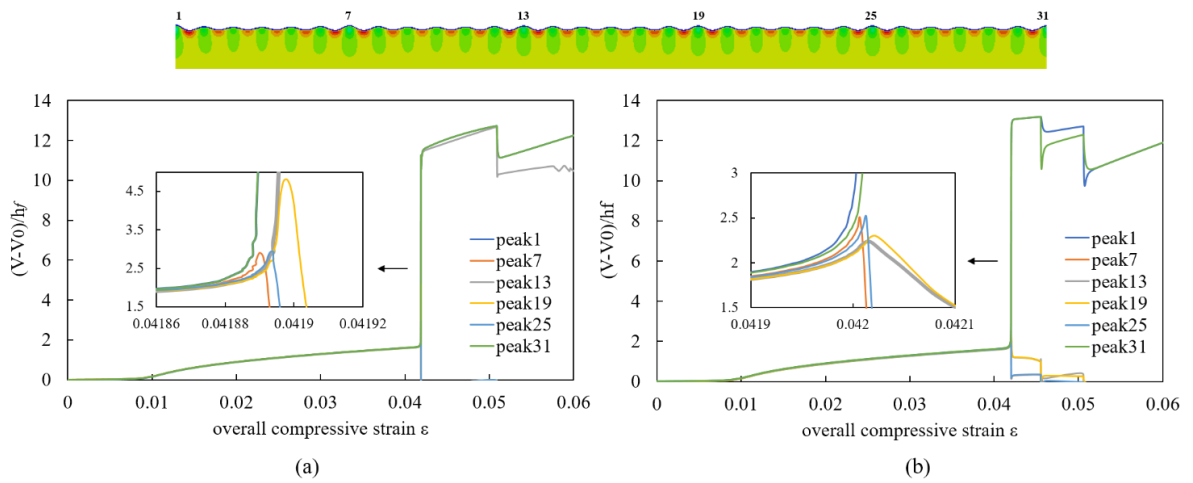

Fig.17 ridge formation and growth process with $\lambda_0 = 2.0$, (a)damping factor $\beta = 0.0002$; (b) $\beta = 0.0005$.

For the pre-stretch of 2.0, the ridge formation process is similar with the case of pre-stretch of 1.8 and damping=0.0002. When the damping factor takes 0.0002, the 1st, 7th, 13th,19th,25th and 31st wrinkles all arise to develop to the potential ridges. However, during the asynchronous snapping, only the 1st, 13th, and 31st wrinkles actually transition to the ridges, and the other 3 potential wrinkles are flattened. When the damping factor is 0.0005, the 1st, 7th, 13th,19th,25th and 31st wrinkles also all arise to become the potential ridges, but finally only the 1st and 31st wrinkles successfully snap to stable ridge state.

From the above detailed analysis on wrinkling to ridge snapping process, it is found that at the very early stage when the wrinkles develop to the potential ridges, the potential ridges are always arranged at the period which has the smallest critical strain $\varepsilon_{w \to r}$. However, the snapping process of these potential ridges are not strictly synchronized due to all kinds of perturbation and imperfection. If all these potential ridges complete the snapping process, then the formed ridges will be periodic and ordered, such as the case of $\lambda_0 = 1.7$ with β =0.0002 or 0.0005 and the case of $\lambda_0 = 1.8$ with β =0.0002 , otherwise the formed ridges will be disordered, such as the case of $\lambda_0 = 1.8$ with β =0.0005 and the case of $\lambda_0 = 2.0$ with β =0.0002 or 0.0005. The system with larger pre-stretch would be more sensitive to the perturbation and imperfection, thus it is harder to generate ordered ridges.

4. Conclusion

In summary, the results can be briefly summarized as follows:

(1) The formation of ridges is the result of the combined action of pre-stretch and overall compression on the nonlinear mechanical behavior of the system. With increasing overall compression, the behavior to generate outward displacement of the wrinkles is first softened and then hardened, therefore there exists a most softened extent. The most softened extent determines whether there exist multiple equilibrium solutions (wrinkles or ridges), thus determines whether the ridges form spontaneously. Pre-stretch softens the behavior to generate outward displacement of the wrinkles. Beyond a certain

critical pre-stretch λ_r, during the increasing overall compression, the system has been softened enough, then the ridge solution appears, thus the initial ridge formation happens. With larger pre-stretch, the softening effect is more significant, thus the critical overall compression strain $\varepsilon_{w \to r}$ decreases with pre-stretch.

(2) At the early stage of initial ridge formation, some wrinkles will arise to develop to potential ridges, and the potential ridges are always arranged periodically. The periodicity is the result of the configurational force of the translationally symmetry wrinkling surface. Ridge formation can happen with various period, and the critical compressive strain $\varepsilon_{w \to r}$ corresponding to each period is different. In practice, the potential ridges are always formed with the period corresponding to the smallest critical compressive strain $\varepsilon_{w \to r, \min}$.

(3) During the initial ridge formation process, the snapping of these potential ridges is not strictly synchronized due to all kinds of perturbation and imperfection. If all these potential ridges complete the snapping process, then the formed ridges will be periodic and ordered, otherwise the formed ridges will be disordered. The system with larger pre-stretch would be more sensitive to the perturbation and imperfection. Therefore, With smaller pre-stretch, it is easier to generate periodic ridges; otherwise, the system is apt to form disordered ridges.

References